SUB | NIEDERSÄCHSISCHE STAATS- UND UNIVERSITÄTSBIBLIOTHEK GÖTTINGEN

## Werk

**Jahr:** 1983
**Kollektion:** fid.geo
**Signatur:** 8 Z NAT 2148:52
**Digitalisiert:** Niedersächsische Staats- und Universitätsbibliothek Göttingen
**Werk Id:** PPN1015067948_0052
**PURL:** http://resolver.sub.uni-goettingen.de/purl?PPN1015067948_0052

**LOG Id:** LOG_0042
**LOG Titel:** Energetic particle signatures near magnetospheric boundaries
**LOG Typ:** article

## Übergeordnetes Werk

**Werk Id:** PPN1015067948
**PURL:** http://resolver.sub.uni-goettingen.de/purl?PPN1015067948
**OPAC:** http://opac.sub.uni-goettingen.de/DB=1/PPN?PPN=1015067948

## Terms and Conditions

The Goettingen State and University Library provides access to digitized documents strictly for noncommercial educational, research and private purposes and makes no warranty with regard to their use for other purposes. Some of our collections are protected by copyright. Publication and/or broadcast in any form (including electronic) requires prior written permission from the Goettingen State- and University Library.
Each copy of any part of this document must contain there Terms and Conditions. With the usage of the library's online system to access or download a digitized document you accept the Terms and Conditions.
Reproductions of material on the web site may not be made for or donated to other repositories, nor may be further reproduced without written permission from the Goettingen State- and University Library.

For reproduction requests and permissions, please contact us. If citing materials, please give proper attribution of the source.

## Contact

Niedersächsische Staats- und Universitätsbibliothek Göttingen
Georg-August-Universität Göttingen
Platz der Göttinger Sieben 1
37073 Göttingen
Germany
Email: gdz@sub.uni-goettingen.de

J Geophys (1983) 52:176–189

Journal of Geophysics

*Review Article*

# Energetic Particle Signatures Near Magnetospheric Boundaries*

M. Scholer
Max-Planck-Institut für Physik und Astrophysik, Institut für extraterrestrische Physik, 8046 Garching, Federal Republic of Germany

**Abstract.** Two aspects of magnetospheric energetic particles have gained increasing attention in recent years: firstly their signatures, in particular the anisotropy, have been used in order to study the behaviour of magnetospheric boundaries, and secondly the particles themselves have been analyzed in order to determine their acceleration mechanism. The first aspect is particularly useful when studying the structure and the temporal behaviour of the magnetopause and when investigating such processes as reconnection. The acceleration of particles has been found to be important at the boundary of the plasma sheet. This paper presents a review of recent ISEE observations of energetic ions and electrons near the magnetopause and near the boundary of the plasma sheet.

**Key words:** Magnetospheric boundaries – Magnetospheric energetic particles – Magnetopause – Plasma sheet

## Introduction

The behaviour of energetic particles in the outer magnetosphere has been studied extensively for two decades. In particular, observations of these particles have been used in order to determine their acceleration sites, but they have also been used as remote sensors in order to probe magnetospheric boundaries, as the magnetopause and the plasma-sheet boundary. Spurred on by the high-quality data returned from the ISEE satellites the topic of energetic particles near magnetospheric boundaries has gained new interest. In this report, we will review recent progress made on the structure of the magnetopause and the plasmasheet boundary layer utilizing ISEE energetic particle observations.

## Density Gradients Near Magnetopause and Remote Sensing

Due to their large gyroradius, energetic ions are ideally suited to probe magnetospheric boundaries to large distances from the satellite, i.e. up to two gyroradii. This concept has first been applied successfully near the magnetopause by Konradi and Kaufmann (1965) and Kaufmann and Konradi (1969; 1973). Assuming the magnetopause to be a perfectly absorbing boundary, Williams (1979a, 1980) has analyzed ISEE 1 three dimensional energetic particle distributions to infer magnetopause distances, orientations, and velocities. The concept is shown schematically in Fig. 1, taken from a paper by Fritz and Fahnenstiel (1982). Let us assume that the magnetic field points in the $z$ direction in a GSE (geogentric solar equatorial) coordinate system. A detector scanning in the ecliptic plane is measuring an azimuthal ion distribution as shown in Fig. 1a as the dark line.

The azimuthal scan exhibits a large anisotropy indicating that the satellite is close i.e. within two gyroradii of a strong particle density gradient. Superimposed is a square

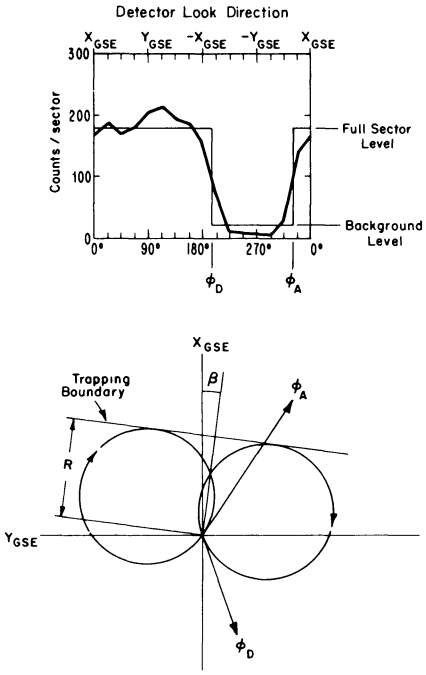


**Fig. 1.** Technique for determining trapping boundary parameters near the subsolar magnetopause. At the top of the figure is the 16 sector normalized partially-trapped >24 keV ion distribution. Superimposed is a square wave fit from which the angles $\varphi_D$ and $\varphi_A$ are obtained. The drop in count rate from $\varphi_D$ to $\varphi_A$ is interpreted as scattering from a trapping boundary as shown in the lower portion of the figure. From these angles, the perpendicular distance $R$ and orientation angle $\beta$ to the trapping boundary are obtained (Fritz and Fahnenstiel, 1982)

* Based on an invited review paper given at the Symposium on Plasma and Energetic Particles in the Magnetosphere, EGS Meeting, 23–27 August 1982, Leeds, U.K.

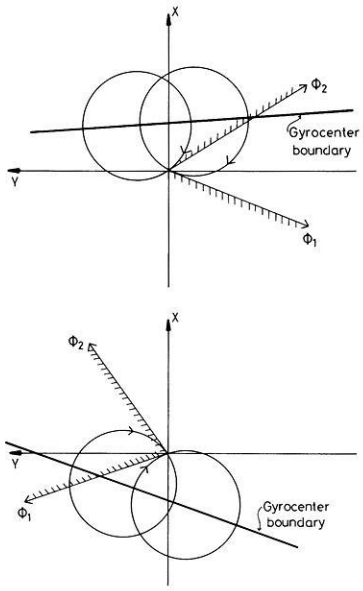


**Fig. 2.** Schematic representation of the sensing of a sharp gradient in gyrocenter density from the inside (upper part) and outside (lower part) of the particle distribution

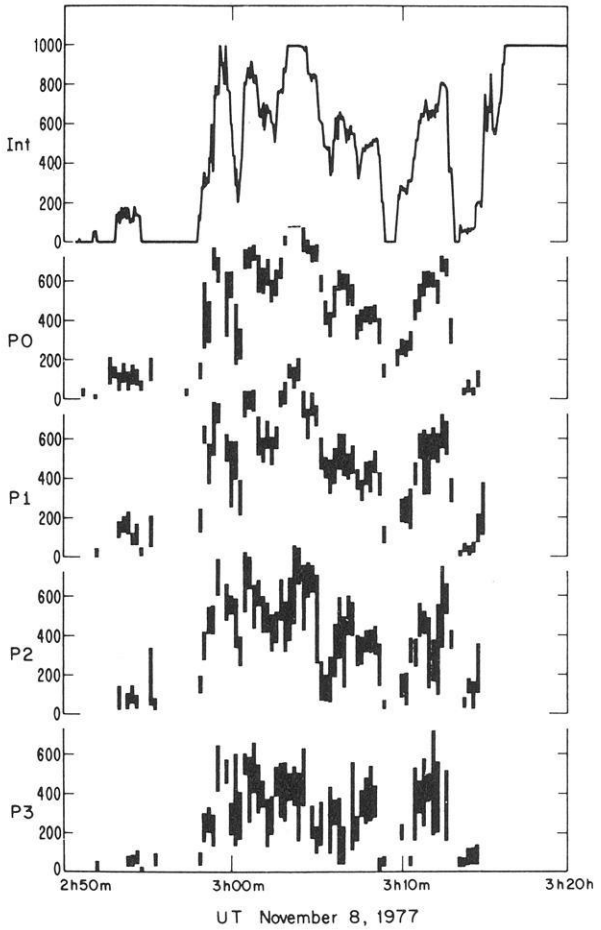


**Fig. 3.** Comparative trapping boundary distances. The distances to the trapping boundary computed for each energy channel are plotted as a function of time. P0-P3 channels have 15 s resolution. The integral >24 keV channel has 4 s resolution and error bars have been omitted for clarity (Fritz and Fahnenstiel, 1982)

wave fit from which the angles $\varphi_A$ and $\varphi_D$ are derived. These angles are interpreted as the arrival directions at the satellite of the last magnetospheric particles which are completing their gyromotion without contacting the absorbing boundary. This geometry is depicted in Fig. 1b, where it is seen that particles with arrival directions counter clockwise from $\varphi_A$ to $\varphi_D$ can complete their gyroorbits while those from $\varphi_D$ to $\varphi_A$ will contact the boundary and are absorbed. The angles $\varphi_D$ and $\varphi_A$ allow a unique determination of the perpendicular distance $R$ and orientation angle $\beta$ to the plane absorbing boundary. Williams (1979a) has assumed the magnetopause itself to be the absorbing boundary, although Williams (1980) cautioned that such an identification of the magnetopause is only valid in the sense that one is identifying the last magnetic field line which contains a trapped type particle distribution. Therefore, Fritz and Fahnenstiel call this boundary the trapping boundary and there are indeed cases in Williams (1980) where this boundary is earthward of the magnetopause as determined from the magnetic field measurements (e.g., 4 December 1977 magnetopause crossing).

We should like to avoid the concept of an absorbing boundary altogether and refer instead to the sensing of a sharp density gradient. We have to be more specific and differentiate between a gradient in number density and a gradient in gyrocenter density. Figure 2 shows schematically the sensing of a sharp gradient of the gyrocenter density. Let us assume the magnetic field is in the $z$-direction and there are no particles with a gyrocenter sunward (positive $x$-direction) of the gyrocenter boundary. The satellite is at the center of the coordinate system. Particles with arrival directions $\varphi_1$ and $\varphi_2$ are particles whose gyrocenters are just inside the gyrocenter boundary. Particles with arrival directions clockwise from $\varphi_1$ to $\varphi_2$ have their gyrocenter earthward of the gyrocenter boundary. Particles with arrival directions counter clockwise from $\varphi_1$ to $\varphi_2$ must have their gyrocenters sunward of the gyrocenter boundary and as the gyrocenter density is zero here, these arrival directions are empty. The lower frame of Fig. 2 shows that the satellite is observing particles at certain arrival directions even if it is outside of the region of gyrocenter density, i.e. the satellite is probing the boundary from the outside. The distance to this boundary is half the distance to the absorbing boundary introduced in Fig. 1. It may well be that this sharp gradient in gyrocenter density is due to an absorbing boundary (magnetopause, last closed field line, etc.), but this is not necessarily so.

Fritz and Fahnenstiel (1982) found that the plasma boundary layer occasionally penetrates up to several hundred kilometers earthward of the trapping boundary as determined by energetic ions. If the trapping boundary determines the position of the last closed field line, the occurrence of magnetosheath plasma earthward of the trapping boundary would be inconsistent with current merging theories. However, the last closed field line is probably determined more closely by the gyrocenter boundary introduced above. This boundary is one gyroradius earthward of the trapping boundary introduced by Fritz and Fahnenstiel, so that there would be no overlap between boundary layer and closed field lines.

The investigations of Williams (1979a, 1980) and Fritz and Fahnenstiel (1982) revealed the existence of 100–400 s waves with amplitudes of a few hundred kilometers of the trapping boundary and, by inference, of the magnetopause.

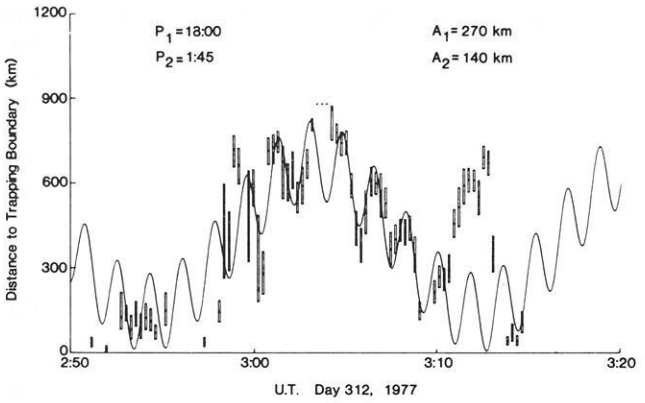


**Fig. 4.** Periodicity in R. A double period sinusoid with periods of 105 s and 18 min and amplitudes of 140 km and 270 km is superimposed on the trapping boundary distances obtained for the P0 channel. The 105 s periodicity is identified with waves on the boundary, while the 18 min component is used to fit an apparent inward "breathing" mode motion (Fritz and Fahnenstiel, 1982)

Figure 3, taken from Fritz and Fahnenstiel (1982), shows for a particular inbound magnetopause crossing of ISEE 2 the distance from the satellite to the trapping boundary as derived from the remote sensing with ions of different energies. The energy bins are labeled P0 to P3 and range from $>24$–$\sim 70$ keV. The channel labeled Int is an integral channel above 24 keV. One can clearly see the oscillatory motion of the trapping boundary. In order to derive the periodicities in $R$, Fritz and Fahnenstiel have fitted a double period sinusoid to the data of Fig. 3. The result is shown in Fig. 4. The periods of the sinusoids are 105 s and 18 min, with amplitudes of 140 km and 270 km. The authors suggest that the 105 s periodicity is due to waves on the boundary whereas the 18 min periodicity is a "breathing" motion of the magnetopause as a whole. The concept of a wavy structure of the trapping boundary is supported by two more observations: Williams (1980) has shown that the orientation angle $\beta$ (defined as a clockwise rotation of the tangent to the magnetopause in the $X_{SE}$, $Y_{SE}$ plane from the $-Y_{SE}$ axis) shows significant variations. Figure 5 from Williams (1980) shows for five magnetopause crossings the orientation angle versus time for consecutive 1-min intervals as indicated. Also shown are suggested periodic variations with the respective period in seconds. Figure 5 shows the regular presence of variations in the orientation angle of the trapping boundary which are consistent with boundary waves in the few hundred second period range. A second observation suggesting a wavy structure of the boundary is the different boundary distance obtained from the sounding with different ion energies. As can be seen from Fig. 3, distances obtained with high energy ions (P3) are consistently lower than distances obtained from low energy ions ($>24$ keV). Fahnenstiel (1981) has suggested that in the case of a wave geometry, the aspect ratio of the wave could be such that the trough of the wave is accessible to the smaller gyroradius ions, whereas the higher energy ions come into contact with the wave crest. This is shown schematically in Fig. 6.

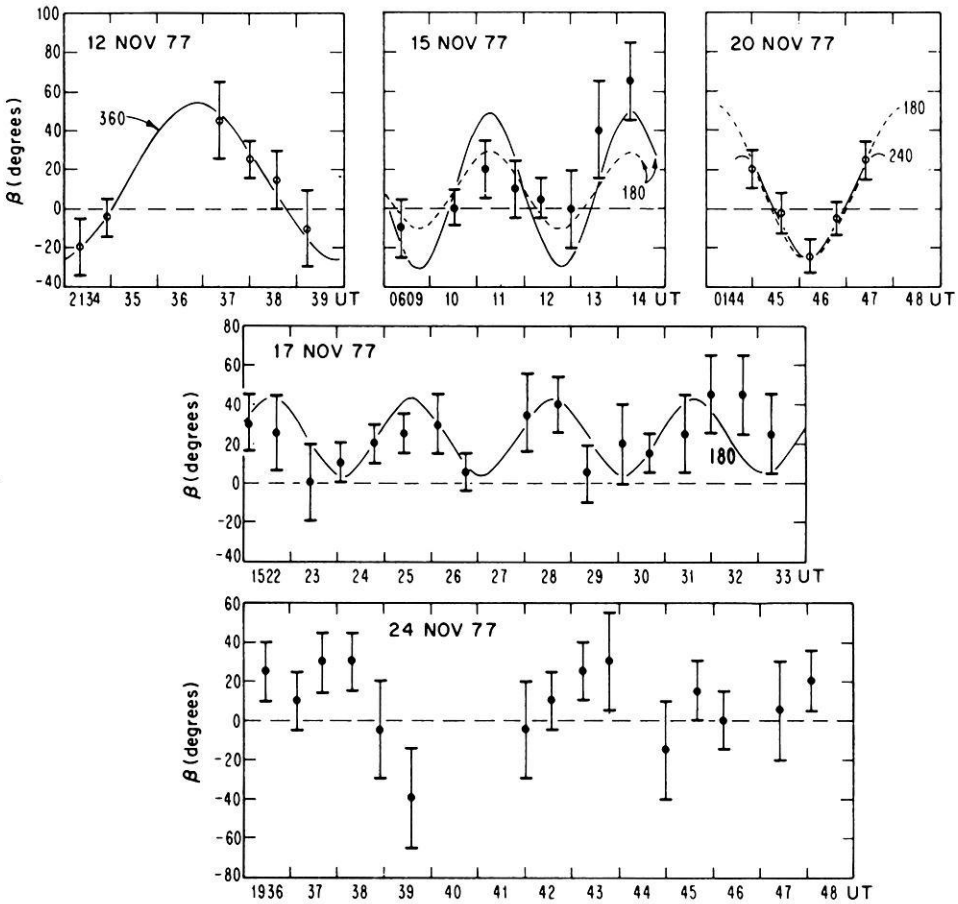


**Fig. 5.** Five time intervals for which nearly contiguous determinations of the magnetopause orientation angle could be made. $\beta$ is plotted versus time for consecutive 1-min intervals as indicated. Periodic variations with the indicated period in seconds are shown for reference. Two amplitudes at a 180-s period are shown in the 15 November 1977 panel (Williams, 1980)

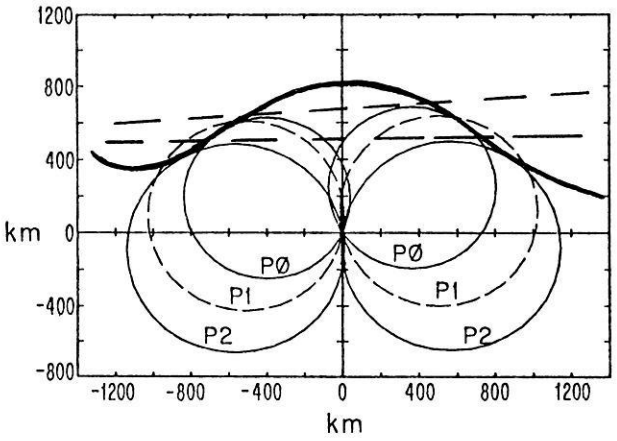


**Fig. 6.** Sounding of the wave crest and trough at the magnetopause by ions with different gyroradii (Fahnenstiel, 1981)

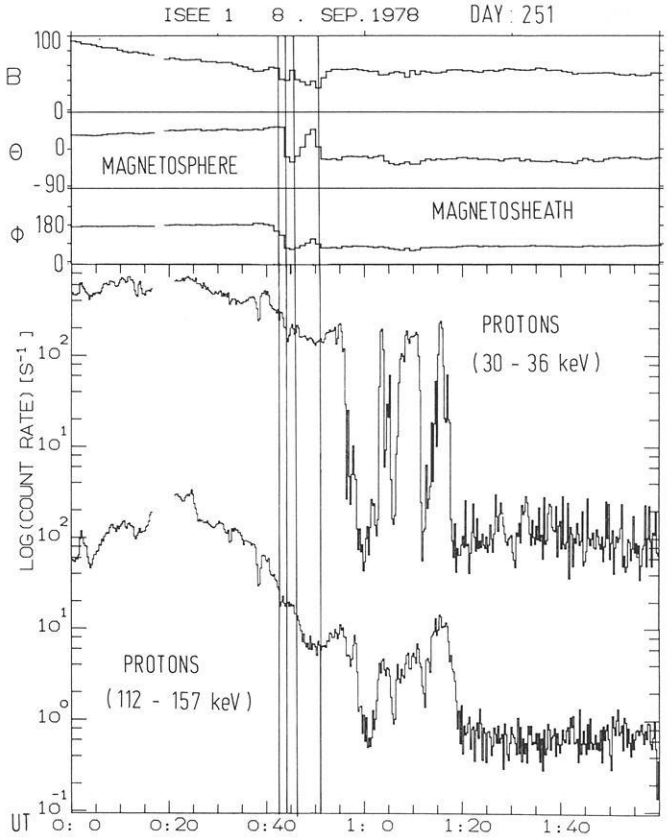


**Fig. 7.** Time behaviour of magnetic field magnitude and direction during a magnetopause crossing (three top panels) and time profile of 30–36-keV and 112–157-keV protons (bottom panel). Between the first two and the second two vertical lines a magnetopause is identified from magnetic field and plasma data (Scholer et al., 1981)

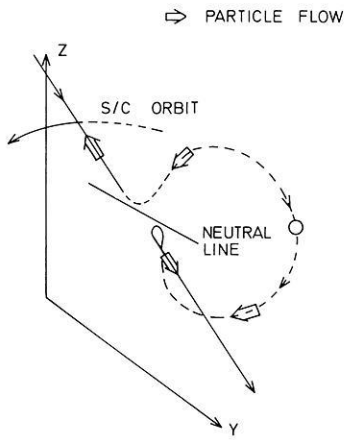


**Fig. 8.** Schematic representation of an interplanetary magnetic field line reconnected to a field line of the Earth's dipole and corresponding outflow of magnetospheric particles (Scholer et al., 1981)

## Energetic Particles and Reconnection

Energetic ions are often found to constitute a layer outside of the magnetopause. Williams (1979b), Richter et al. (1979) and Lanzerotti et al. (1979) reported the existence of an energetic ion layer outside the magnetopause. Recently, Scholer et al. (1981) investigated energetic particle behaviour during magnetopause crossings which have been identified by Sonnerup et al. (1981) as reconnection events, i.e. where the rate of change of the tangential momentum of the plasma as it flows across the magnetopause layer is equal to the net tangential Maxwell stress. Figure 7 shows the time behaviour of the magnetic field (magnitude and direction) and of the energetic protons during an outbound magnetopause crossing on 8 September 1978 as shown in Scholer et al. (1981). It can be seen that the energetic particle population extends well within the magnetosheath. In addition the satellite encounters several burst-like energetic particle events in the magnetosheath. Before interpreting these observations we would like to discuss what a satellite should observe near a magnetopause which is a rotational discontinuity. A satellite crossing the magnetopause above or below an $x$-type neutral line will encounter reconnected field lines up to the outer reconnection separatrix. If magnetospheric trapped particles are escaping along the reconnected field lines, they should be observable up to the separatrix, which is on the magnetosheath side of the magnetopause. Scholer et al. (1981) interpreted there observations of energetic ions outside the magnetopause as a crossing of the region between magnetopause and outer separatrix. Figure 8 is a schematic representation of an interplanetary magnetic field line reconnected to a field line of the Earth's dipole. If magnetospheric particles escape along reconnected field lines a satellite crossing the reconnection region above the neutral line should observe particles streaming antiparallel to the magnetosheath field and a satellite crossing below the neutral line should observe particles streaming parallel to the magnetosheath field. This is indeed observed: Fig. 9 shows spatial distributions in the ecliptic together with the projection of the magnetic field. Outside the magnetosphere (e.g. 044:58–045:14 UT) the particles are streaming antiparallel to the field consistent with a reconnection line south of the satellite as determined from the plasma measurements by Paschmann et al. (1979) (note that Fig. 9 shows the intensity in the instrument look direction). Sonnerup et al. (1981) have shown that when the satellite is crossing south of the reconnection line particles are indeed streaming parallel to the field.

Williams and Frank (1980) presented indirect evidence for open field lines within the magnetosphere. They found field-aligned asymmetries in the energetic ion distributions at satellite positions inside the magnetosphere close to the

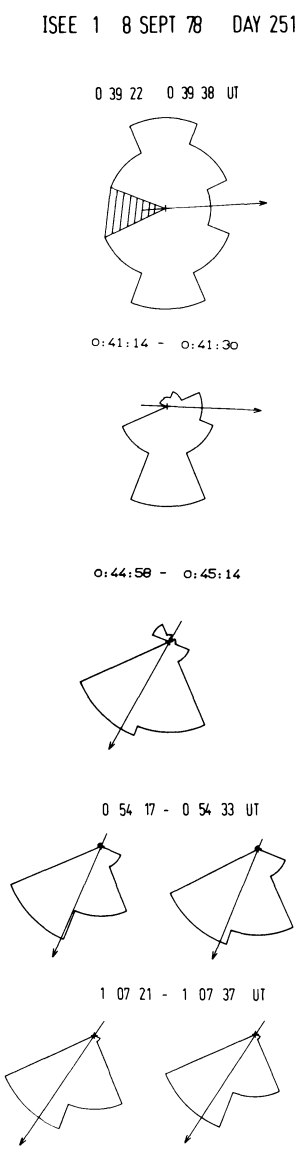


**Fig. 9.** Energetic proton (~30 keV) distributions observed at three different times (from top to bottom: within the magnetosphere, in the layer outside the magnetopause, and in a magnetosheath burst). The distributions to the right are Compton-Getting-transformed into a coordinate system moving with the component of the magnetosheath plasma velocity perpendicular to the magnetic field. Arrows indicate the projection of the magnetic field into the ecliptic. The Sun is to the left of the figure (Scholer et al., 1981)

magnetopause. Scholer et al. (1982a) re-examined the 8 September 1978 event in order to determine the field line topology inside the magnetopause. When the satellite approached the magnetopause from the inside they first observed trapped distributions between certain look phases and missing particles at the other phases with respect to the local magnetic field. This indicates that the spacecraft is inside the last closed field line, but within 2 gyroradii of it. The following three-dimensional scan (each scan of the instrument takes 36 s) shows no particles at certain phase angles, at the other phase angles the particles in the 60°–90° pitch angle range are depleted, so that the field line passing through the satellite is unable to mirror and trap these ions below the satellite. However, as also emphasized by Eastman and Frank (1982), before and even for some time after the magnetopause crossing of 8 September 1977 the energetic electrons exhibit a pancake like distribution (i.e. peaked at a pitch angle of 90°), indicating a trapped population and thus closed field lines.

Daly and Fritz (1982) have solved this apparent puzzle and have shown how trapped-like electrons can be maintained on open field lines together with streaming ions. They have investigated the idea that the electrons could be trapped by magnetic mirroring from the increased field in the magnetosheath. Figure 10 from Daly and Fritz (1982) shows the total magnetic field plotted against time around the magnetopause crossing (which at ISEE 2 occurred during a data gap). Also indicated are times of streaming ions and electrons. The magnetic field is seen to have a minimum shortly before the magnetopause crossing and increases again in the magnetosheath. Assuming a maximum magnetosheath field strength of $B_m = 59$ nT for all field lines crossed by the satellite Daly and Fritz (1982) converted all values of $B < B_m$ into an angle $\alpha$, that represents the edge of the expected loss cone in that field. This angle is shown on the right of Fig. 10. No particles are expected at a pitch angle less than $\alpha$, particles between $\alpha$ and 90° are returning from the magnetosheath after mirroring, particles between 90° and 180°-$\alpha$ are coming from the magnetosphere and will be reflected back and particles above 180°-$\alpha$ can come from a source deeper in the magnetosphere and will be lost in the magnetosheath. Measured upper and lower cutoff angles in the electron distributions as shown in Fig. 10 indeed follow the field strength curve rather closely. Figure 11 is a reconstruction of the field line geometry proposed by Daly and Fritz (1982). The vertical line in the middle is the magnetopause and the bars between some of the field lines indicate the mirroring points for those particles with a pitch angle of 90° in the steady magnetosheath field. These particles are trapped on the field line between the bars, i.e. the satellite will observe close to the magnetopause inside as well as outside a trapped electron distribution. The reason that energetic protons are not similarily trapped is their much larger (43 times greater) gyroradius. In a field of 55 nT, 36 keV protons have a gyroradius of 500 km which is of the same order as the thickness of the magnetopause current layer as determined by Russell and Elphic (1978). It is thus unlikely that the ions can follow the bend in the field line adiabatically, so that the mirror hypothesis does not apply.

Magnetosheath particles are not only transmitted into the magnetosphere and thus form the boundary layer but they can also be reflected due to interaction with the current layer. Sonnerup et al. (1981) found that some magnetosheath particles are accelerated in the magnetopause layer and are reflected back into the magnetosheath, forming a population having ~20% of the total sheath density just outside the current layer. Similarily, energetic magnetospheric ions can be accelerated in the current layer and are reflected back into the magnetosphere. Scholer and Ipavich (submitted 1983) have presented some evidence for the acceleration and reflection of energetic ring current ions at the magnetopause. Figure 12 shows 64-s-averaged spatial distributions of energetic protons around the final magnetopause crossing on 5 July 1978. These distributions are measured in the ecliptic plane; the Sun is to the left of the figure and the intensity is plotted in the instrument look direction. From the plasma and magnetic field data it has

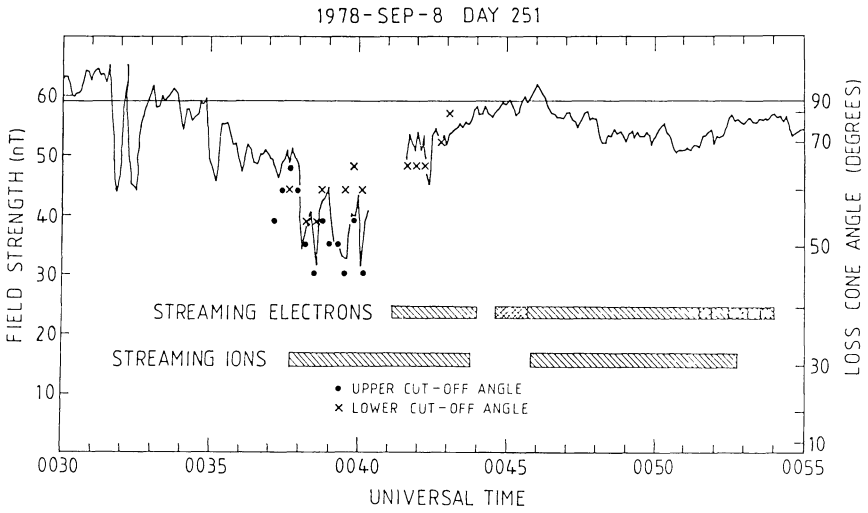


**Fig. 10.** Total magnetic field plotted against time, from 0030 to 0055 UT on 8 September 1978. On the left is the magnetic field scale, on the right the corresponding loss cone angle based on a mirroring field of 59 nT Also indicated are times of streaming ions and electrons; the times of heavier shading for the electrons indicate very intense streaming. Measured upper and lower cutoff angles in the electron distributions are also plotted via use of the angle scale on the right (Daly and Fritz, 1982)

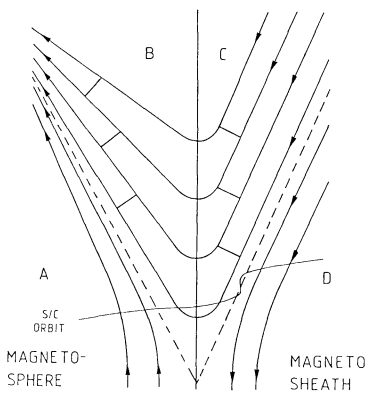


**Fig. 11.** Reconstruction of the field line geometry and spacecraft trajectory. The vertical line in the middle is the magnetopause, the lines with arrows are field lines. The bars between some of the field lines indicate the mirroring points for those particles with a pitch angle of 90° in the steady magnetosheath field, these particles are trapped on the field line between the bars. A horizontal curve represents the spacecraft's trajectory. The dashed lines and the magnetopause separate regions *A, B, C,* and *D* of different field line topology (Daly and Fritz, 1982)

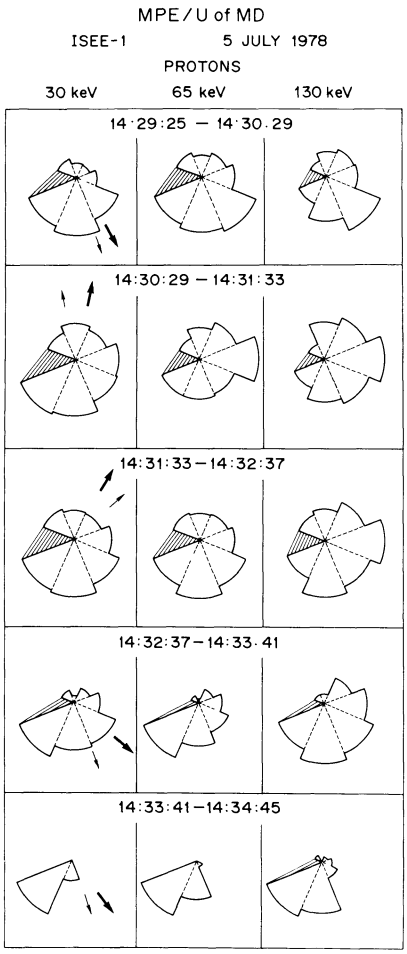


**Fig. 12.** Consecutive 64 s-averaged spatial distributions of ~30 keV, ~65 keV, and ~130 keV protons in the ecliptic plane during a multiple magnetopause crossing. The Sun is to the left of the Figure, the Sun sector is shaded. Also shown is the projection of the magnetic field into the ecliptic plane (light arrow) as well as the projection of the velocity vector (heavy arrow) into that plane (Scholer and Ipavich, 1983)

been established that the satellite was north of a possible *x*-type neutral line (Sonnerup et al., 1981). As outlined above the satellite should observed inside the magnetosphere, i.e. when the magnetic field is pointing from dusk to dawn (light arrow), a streaming of the magnetospheric particles out of the magnetosphere antiparallel to the magnetic field. The anisotropies are, however, opposite to those expected from the simple picture of magnetospheric particles leaking out along open field lines. Scholer and Ipavich (submitted 1983) suggested that part of the magnetospheric ions are reflected and accelerated at the magnetopause current layer so that at a constant energy one might observe higher fluxes of particles streaming away from the current layer parallel to the field than towards the current layer antiparallel to the field. Figure 13 from Scholer and Ipavich shows, to the left, phase space densities of protons antiparallel to the magnetic field within the magnetosphere. Let us assume that the open flux tubes contract over the magnetopause at the speed $V_F$. In a system moving with velocity $V_F$ particles gain or lose no energy during reflection and transmission since there is no electric field and the field lines are at rest. The distribution of the reflected particles is then found by constructing the mirror image of the input distribution about the field line speed multiplied with the

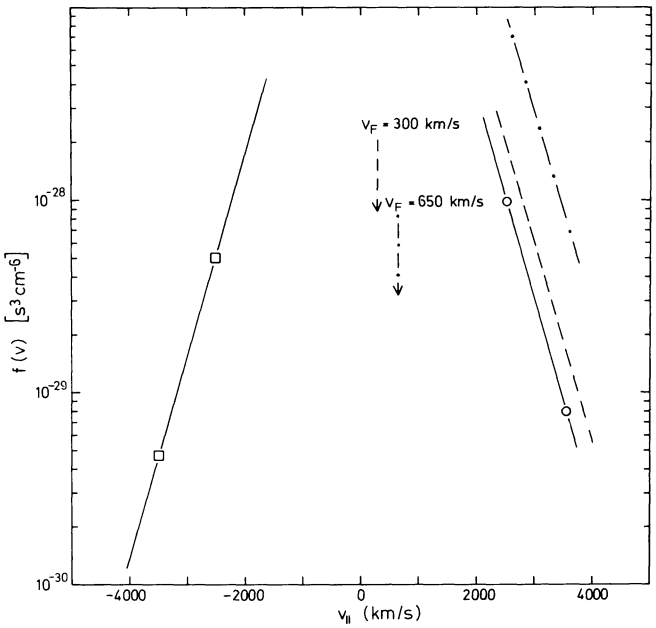


**Fig. 13.** Open squares: phase densities of protons antiparallel to the magnetic field. Dashed distribution results from the solid distribution by mirroring at $v_F = 300$ km/s, dashed-dotted distribution results by mirroring at 650 km/s. Open circles are measured phase space densities parallel to the field and can be obtained from dashed-dotted distribution by multiplying with 0.1 or from dashed distribution by multiplying with 0.5, respectively (Scholer and Ipavich, 1983)

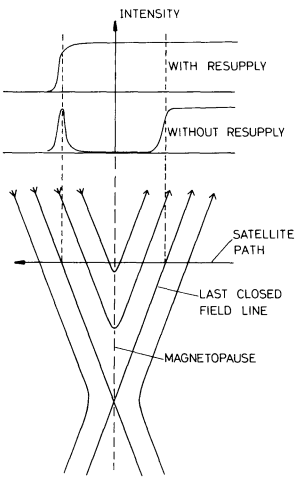


**Fig. 14.** Schematic representation of the reconnection configuration at the magnetopause. At the top are shown particle intensity profiles as measured during a satellite crossing if there is either resupply or no resupply of particles on open field lines

reflection coefficient. Figure 13 shows distributions mirrored at 300 km/s (dashed) and 650 km/s (dashed-dotted). Assuming either 50% or 10% reflection efficiency one can easily obtain the measured phase space densities of particles flowing within the magnetosphere away from the current layer (open squares).

Before leaving the subject of steady state reconnection at the magnetopause it should be emphasized that magnetospheric particles have to be continuously replenished on open field lines. Scholer et al. (1981) noted that a field line should be empty after reconnection within two bounce periods i.e. within approximately 1 min. A satellite crossing outbound, north of a neutral line should essentially observe particles up to the inner separatrix, no particles between inner and outer separatrix and an intensity increase close to the outer separatrix. This is shown schematically in Fig. 14. Since such a drop in intensity is never observed, but the profiles look rather as at the top of Fig. 14, a rather efficient continuous re-supply mechanism on open field lines must be postulated.

## Flux Transfer Events

A feature found for the first time by the ISEE satellites and associated with the magnetopause are the so-called flux transfer events (FTE's). The FTE's are evident from characteristic signatures in the magnetic field data and have been interpreted by Russell and Elphic (1978; 1979) as magnetic flux tubes interconnected with the magnetospheric field. Daly et al. (1981), Scholer et al. (1982b), and Speiser and Williams (1982) have investigated energetic particle signatures during magnetic flux transfer events. Figure 15 from Scholer et al. (1982b) shows, for a magnetopause crossing on 8 November 1977, from top to bottom, the plasma density, the three components of the magnetic field in the boundary normal system: **N** is the vector outward and normal to the magnetopause, **L** is the GSM (geocentric solar magnetospheric) $z$-axis projected onto the magnetopause, and **M** is given by **NxL**. A positive excursion of the **N** component, followed by a negative excursion before returning to zero, is indicative of magnetic flux transfer events in the magnetosheath. The lower panels show spin-averaged energetic protons and electrons. During the two FTE's from 0212–0215 UT and 0233–0238 UT there are clear particle enhancements of both protons and electrons, although the electron intensity is considerably below the intensity well within the magnetosphere. From the spatial distributions of protons and electrons within the FTE's shown in Fig. 16 it can be seen that the protons are streaming antiparallel to the magnetic field (the projection into the ecliptic is shown by an arrow) whereas the electrons exhibit a more or less isotropic distribution. The ion distributions are consistent with a picture of magnetospheric particles leaking out into a magnetosheath magnetic flux tube which is connected to the magnetospheric field. A qualitative sketch of such a flux tube topology has been given by Speiser and Williams (1982) and is shown in Fig. 17. Speiser and Williams used a one-dimensional, quasi-static model to follow particle orbits from the magnetosphere into the sheath, and map the distribution function using Liouville's theorem. They found good agreement between their model and the observations in the sheath if they assumed the presence of an inward pointing normal magnetic field component and the absence of a tangential electric field. The latter fact may indicate that what one observes in FTE's is the peeling off of a well-defined flux tube that underwent reconnection some time in the past. Speiser and Williams (1982) and Scholer et al. (1982b) observed quasi-trapped (QT) distributions when entering and leaving FTE's. Speiser and Williams (1982) interpreted these QT-distributions as the more slowly outward-moving particles with large pitch angles that get left behind by the faster particles with smaller pitch angles when a flux tube becomes

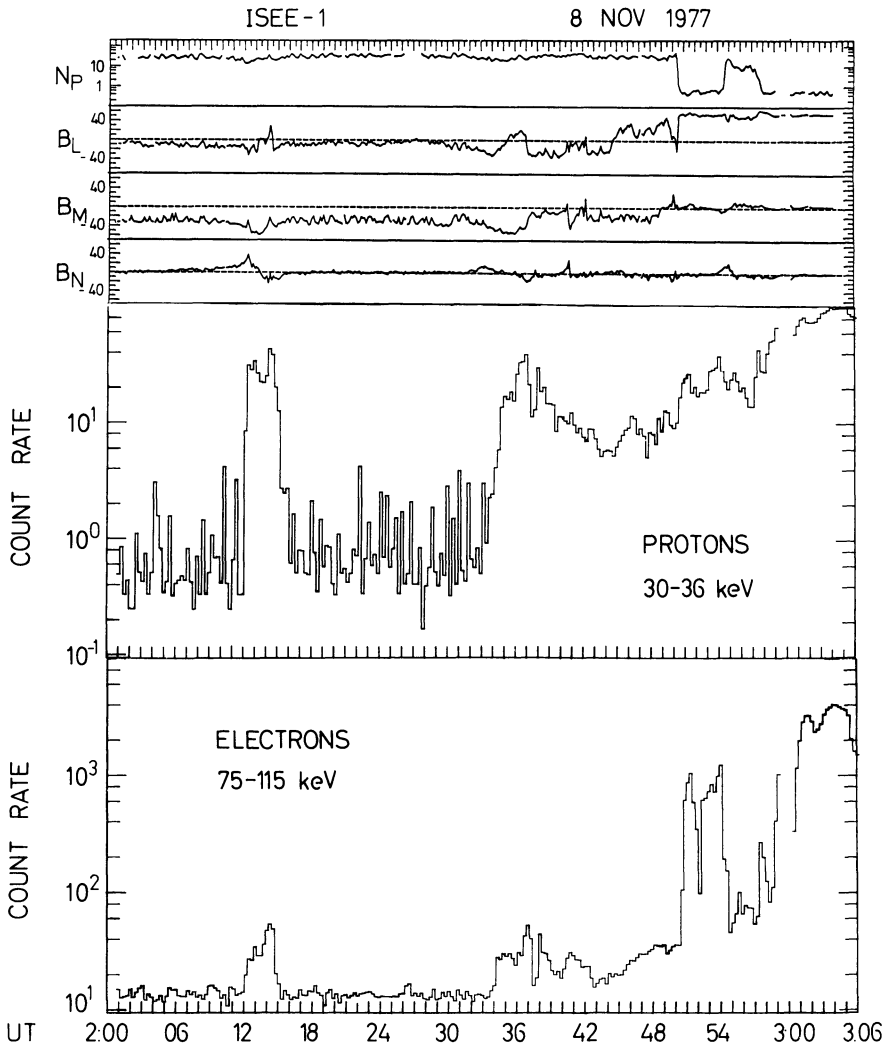


**Fig. 15.** From top to bottom: Plasma density; magnetic field components $B_L$, $B_M$, $B_N$ energetic protons and energetic electrons during the magnetopause crossing on 8 November 1977 (Scholer et al., 1982b)

opened. This implies that the reconnection process is still occurring while one observes the event i.e. one sequentially samples older and younger open field lines when crossing an FTE. Scholer et al. (1982b), on the other hand, claim that they observed particles mainly at 90° pitch angle when entering the flux tube from above as well as when leaving the flux tube below where one should expect to cross freshly opened flux tubes. They suggest that at the boundary of the FTE's the magnetosheath field is draped around the flux tube and may lead to grad $B$ drifts and nonadiabatic particle motion.

Daly and Keppler (1982) have reported that events previously designated inclusion events inside the magnetopause have energetic particle signatures similar to those observed during flux transfer events. Already Williams (1980) identified these events as close encounters of the satellite with the last closed field line. Figure 18 shows energetic particle data (two top panels) and magnetic field data in the boundary normal coordinate system during an inbound magnetopause crossing on 10 November 1977. During the two events in the magnetosphere, at 1503 and 1512 UT, the magnetic field N-component shows negative and positive excursions as during the FTE's in the magnetosheath. The ion intensity decreases somewhat and the pitch angle distribution is such that the ions are steaming antiparallel to the field. The electron intensity drops to the same low level as in the flux transfer events. Daly and Keppler (1982) concluded that these events in the magnetosphere are also flux transfer events viewed from the other side of the magnetopause. This supports the interpretation of flux transfer events as isolated flux tubes in the magnetosphere which connect to the magnetosheath through the magnetopause. Daly and Keppler (1982) have suggested that the same resupply rate for protons and electrons together with the considerably smaller bounce time of the electrons could explain the low levels of electron flux in the FTE's inside and outside the magnetosphere. A different explanation has been given by Scholer et al. (1982b). They argue from the observation of isotropic electron distributions that strong scattering could result in a diffusion type leakage of the electrons along the open flux tubes so that large flux differences between magnetosphere and magnetosheath can be maintained.

Before leaving the subject of energetic particles at the magnetopause we should like to mention the magnetopause energetic electron layer. Such a permanent layer was found by Baker and Stone (1977) along the distant magnetotail and by Meng and Anderson (1975) and Domingo et al. (1977) at high latitudes near the dayside magnetopause and poleward of the polar cusp.

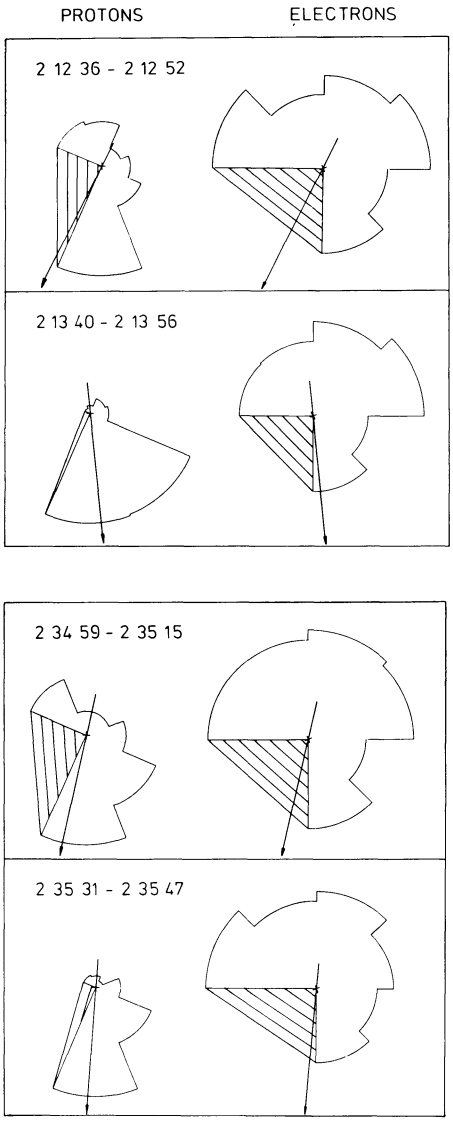


**Fig. 16.** Energetic proton (30–36 keV) and electron (75–115 keV) distributions observed during two flux transfer events on 8 November 1977. The intensity is plotted linearly in the instrument look direction (Scholer et al., 1982b)

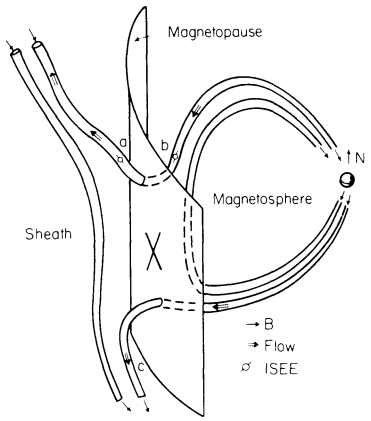


**Fig. 17.** Schematic representation of flow and field directions for flux transfer events (Speiser and Williams, 1982)

## Energetic Ion Observations of the Plasma Sheet Boundary Layer

Energetic ions in the plasma sheet have been studied for many years. Their characteristic features have been used to infer the acceleration site, temporal evolution of the source, net energetic particle transport, electric fields and magnetic field topology. For a recent review on the topic of energetic particle bursts in the Earth's magnetotail see Krimigis and Sarris (1979). Here, we are not concerned with energetic particles in the magnetotail in general but with the recently detected thin layer of non-thermal particles streaming highly collimated along the tail field at the edge of the plasma sheet.

First observations of energetic protons and alpha particles streaming at the edge of the plasma sheet towards the Earth were reported by Möbius et al. (1980). Figure 19, taken from Möbius et al., shows on the left side proton and alpha particle spectra in two sectors of the instrument which is scanning in the ecliptic plane. Angular distributions of ~65 keV/charge protons and alpha particles are shown in the right half of Fig. 19. The sector numbering is such that sector 2 is looking tailward, sector 4 is looking towards dawn, etc. The data are shown consecutively in time from top to bottom, and the angular distribution display shows the counting rate on a linear scale. The particles are streaming predominantly earthward and the spectra of both protons and alpha particles exhibit a maximum of the flux between ~65 and ~130 keV/charge during the first appearance of the particles. Furthermore, the alpha particle layer is confined within the proton layer. The deviation of the anisotropy from the Earth-Sun direction during the first encounter of the plasma sheet energetic ion layer can be explained by the effect of the density gradient perpendicular to the magnetic field at the boundary.

A detailed investigation of the energetic ions at the edge of the plasma sheet has been performed by Williams (1981). The three-dimensional measurements showed strong streaming and beam-like characteristics at each transition from low to high and high to low intensities in the energetic particle population. The azimuthal asymmetries indicate that the energetic ion streaming is located within ~2,000 km of the plasma sheet edge. In general, when encountering the plasma sheet, streaming ions are first observed in the earthward direction at higher energies and the spectrum turns over towards lower energies. Later in the event earthward flowing particles are also observed at lower energies. At the same time as low energy earthward ion jetting is seen, tailward directed fluxes of higher energy ions are detected. These tailward streaming beams are the result of mirror point reflection of the earthward moving ion population. Williams (1981) explained the observation of peaked spectra in terms of a model where a source supplying energetic ions comes in contact with the field line going through the satellite position somewhere tailward of the satellite. Figure 20 from Williams (1981) illustrates the appearance of energetic ion beams at the satellite location due to the propagation of ions from a source with a power law spectrum a distance $d$ away. The left side shows a $E^{-3}$ differential energy spectrum and normalized arrival time ($1/v_{\|} = T/d$, $v_{\|}$ parallel velocity of ion) curves for pitch angles of 0° and 60°. The panels to the right show the time evolution of the spectra observed with an instrument located some distance $d$ away. In this model peaked spectra

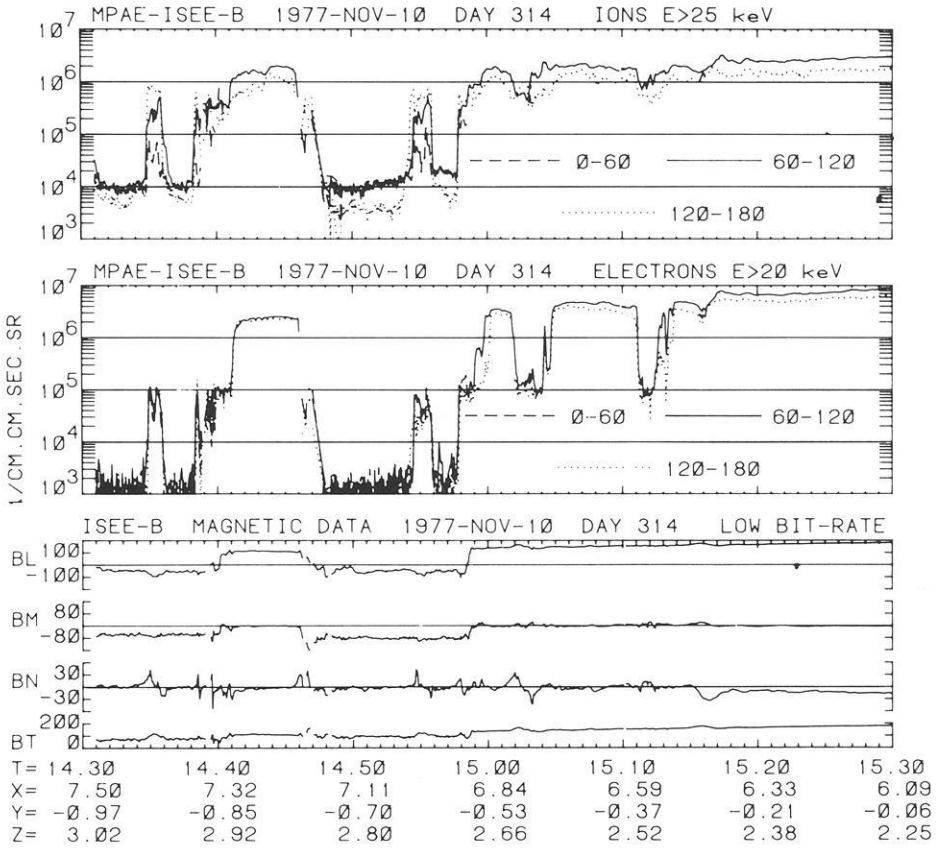


**Fig. 18.** Ion and electron data ($E_i > 25$ keV, $E_e > 20$ keV) plotted against time from 1430–1530 UT on 10 November 1977, and divided into three pitch angle ranges of 60° width each. Inside magnetosphere (1440–1447 and after 1459) the range 0°–60° is not sampled by this detector. The lower panel shows the magnetic field data, in boundary normal components, from Elphic and Russell (1979). *BT* is the magnitude of the field. The unit of field strength is the nano-tesla. The set of four numbers beneath the plot contains the universal time (h and min) and the satellite position (in geocentric solar ecliptic coordinates, in Earth radii) (Daly and Keppler, 1982)

evolving in time and pitch angle are simply due to propagation effects from a time-variable source. Williams (1981) does not propose any specific source mechanism but concludes that the variable nature of the source can be due to a time-variable source, a spatially moving source or random encounters of the spacecraft flux tube with a steady source. This purely kinematical model is illustrated schematically in Fig. 21. Note, however, that while a time-variable source and a spatially moving source can result in the same energy dispersion effects at the satellite position, the spatial structure of the boundary layer is totally different. In the first case (time-variable source) bursts of energetic ions are produced intermittently somewhere in the tail while in the second case (moving source) there are layers of ions with different velocities which will move across the satellite position.

Another explanation of the peaked spectra has been given by Andrews et al. (1981a, b) in terms of the well-known velocity filter effect of a cross-tail electric field. Figure 22a illustrates how this dispersion arises. Field aligned particles of low and high speeds $V_1$ and $V_2$ are ejected from a source $S$ close to the neutral sheet. The **ExB** drift causes both particles to drift down with speed $V_D$ so that their trajectories lie at different angles to the magnetic field **B**. Thus the energetic ions are spatially dispersed such that the most energetic particles lie furthest from the neutral sheet. A satellite moving towards the neutral sheet will observe successively particles to lower and lower energies. Andrews et al. (1981a, b) have combined this velocity dispersion effect with the tailward motion of the source. In Fig. 22b a source moves from position $S_1$ to position $S_2$. During this time particles of slow and high speed ($V_1$ and $V_2$) have reached, under the influence of the **ExB** drift, the end points of the arrows $V_1$ and $V_2$, respectively. The connection of the endpoints of $V_1$ and $V_2$ with the source position $S_2$ then defines upward moving fronts of slow and fast particles. Eventually the satellite will be crossed by these layers of particles of different energy. Figure 22c demonstrates how slow earthward moving particles and fast tailward moving particles can be observed simultaneously. For simplicity we neglect the motion of the source and consider only the **ExB** drift effect. Particles of slow velocity $V_2$ are ejected from a source at position $S$. Their velocity and the **ExB** drift velocity then defines a line $D_2$ where particles with the velocity $V_2$ can be found. Particles of higher velocity $V_1$ can be found at a line $D_1$ further away from the neutral sheet. Let us assume that these particles are adiabatically reflected in the near-Earth magnetic field. They will then move along a line $D_{1r}$ which intersects the line $D_2$ at some location. A satellite at this location will observe simultaneously earthward jetting ions of velocity $V_2$ and tailward moving particles of velocity $V_1$. Due to tailward motion of the source regions with different particle velocity will move across the satellite. Knowing the expansion speed of the boundary, which is due to tailward retreat of the source, the cross-tail electric field can be determined from the timing of the occurrence of ions with different velocities. Andrews et al. (1981b) obtained from a particular plasma sheet boundary crossing of ISEE 2 electric field values between 0.2 and 0.9 mV/m.

Neither Williams (1981) nor Andrews et al. (1981a, b) have suggested any particular source mechanism for the energetic particles. Forbes et al. (1981) studied plasma data

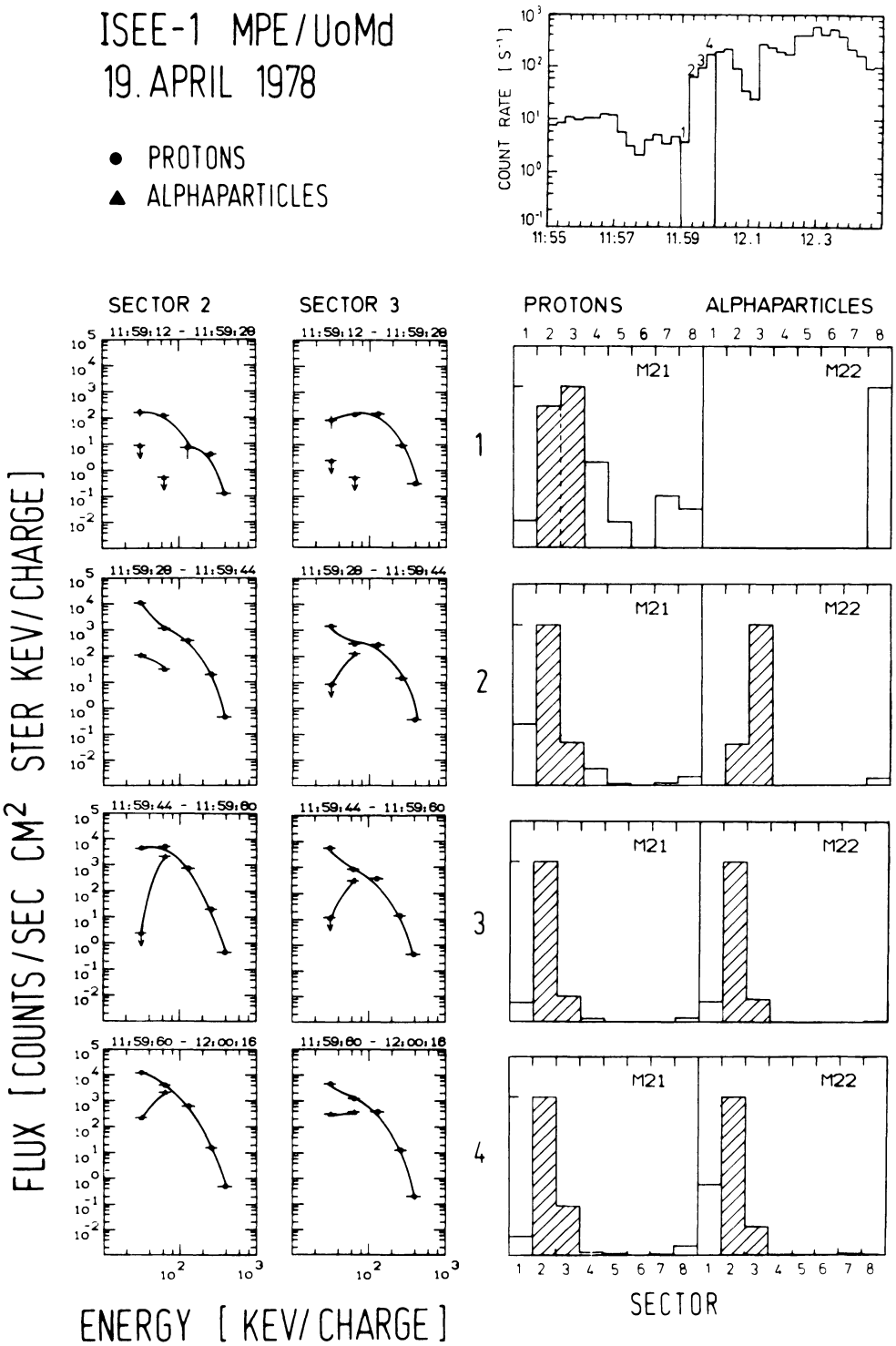


**Fig. 19.** (*Left*) Energy spectra of protons and alpha particles in sectors 2 and 3 together with (*right*) the angular distributions of 60-keV/q protons and alpha particles at the encounter of the plasma sheet (Möbius et al., 1980)

from ISEE 1 and 2 during a crossing of the plasma sheet boundary. They inferred an upward motion of the plasma sheet boundary of $20 \pm 10$ km/s and found at the same time plasma velocities of $\sim 30 \pm 10$ km/s toward the midplane of the plasma sheet. The upward advance of the surface of the plasma sheet in the presence of a downward convective flow induced by a dawn to dusk electric field in the tail requires the tailward motion of an energetic particle source. The source moves onto new magnetic field lines which map progressively deeper into the tail. Forbes et al. (1981) suggest that this motion of the source onto new magnetic field lines is due to the tailward retreat of a magnetic neutral line and that particle acceleration is due to magnetic reconnection.

Andrews et al. (1981a) applied the remote sensing technique with energetic particles to the plasma sheet boundary. They found upward speeds of the plasma sheet expansion of $\sim 50$ km/s. From this, together with the observation of detached flux spikes preceding the main plasma sheet entry, a boundary structure has been proposed where the surface of the plasma sheet is corrugated with boundary waves propagating horizontally. Although the sheet expands slowly

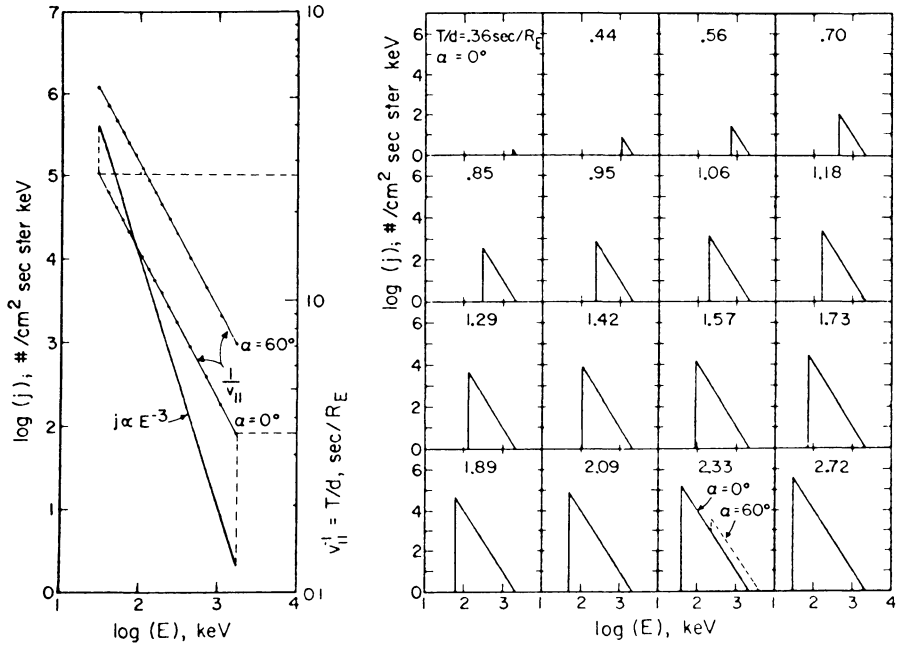


**Fig. 20.** Illustration of the appearance and evolution of "peaked" energy spectra observed by the ISEE 1 medium energy particles instrument due to propagation effects from a representative $E^{-3}$ source. The left panel shows the $E^{-3}$ source along with normalized propagation time, $v_{\|}^{-1} = T/d$, curves for the ISEE 1 instrument. The propagation time curves are shown for pitch angles $\alpha = 0°$ and 60°. The sixteen panels on the right show the time evolution of the instrument response for ions at $\alpha = 0°$ based on propagation from an $E^{-3}$ source an arbitrary distance, $d$, away. Actual arrival times for these spectra are obtained by multiplying the $T/d$ values by the source distance, $d$. One panel shows an $\alpha = 60°$ response for comparison. The concept illustrated by this figure is used with detector sampling characteristics and variable source parameters to explain beams at the plasma edge (Williams, 1981)

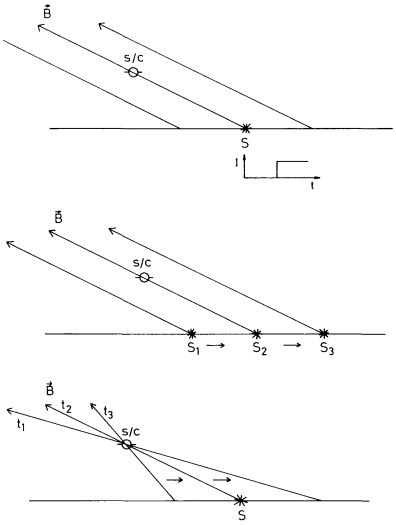


**Fig. 21.** Schematic representation of the occurrence of a time variable source (*top*), a spatially moving source (*middle*) or random encounters of the flux tube through the satellite with a source in the geomagnetic tail

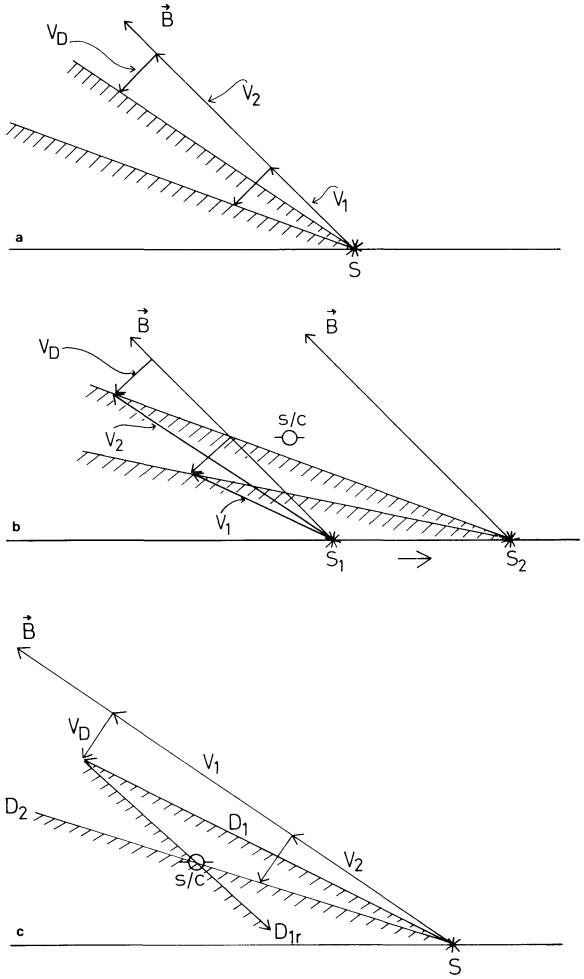


**Fig. 22a.** Diagram to illustrate how the **ExB** drift causes energy dependent boundaries in the tail. **b** Diagram to illustrate how a tailward retreating source together with the **ExB** drift causes upward moving energy dependent boundaries. **c.** Trajectories of particles which can be observed at the satellite when near-earth reflection is included

the large tilt angles produced by the waves can lead to high vertical speed components.

Spjeldvik and Fritz (1981) have reported multiple plasma sheet encounters during an ISEE 1 plasma sheet boundary crossing. Figure 23 shows high resolution ion (24–44.5 keV) and electron (22–39 keV) observations from these authors. Several separate peaks are visible in the ion data and the peaks are typically 2–6 min apart. The ions are characterized by strong spin modulation indicating no observable fluxes when looking earthward and high fluxes when looking tailward. Since the instrument is scanning from north to south and back in 72 s, these peaks are in addition modulated by the scan motion as indicated by the scan position at the bottom of each panel. Only the interior of the last peak shows that the fluxes are essentially isotropic with only a modest spin modulation, i.e. the satel-

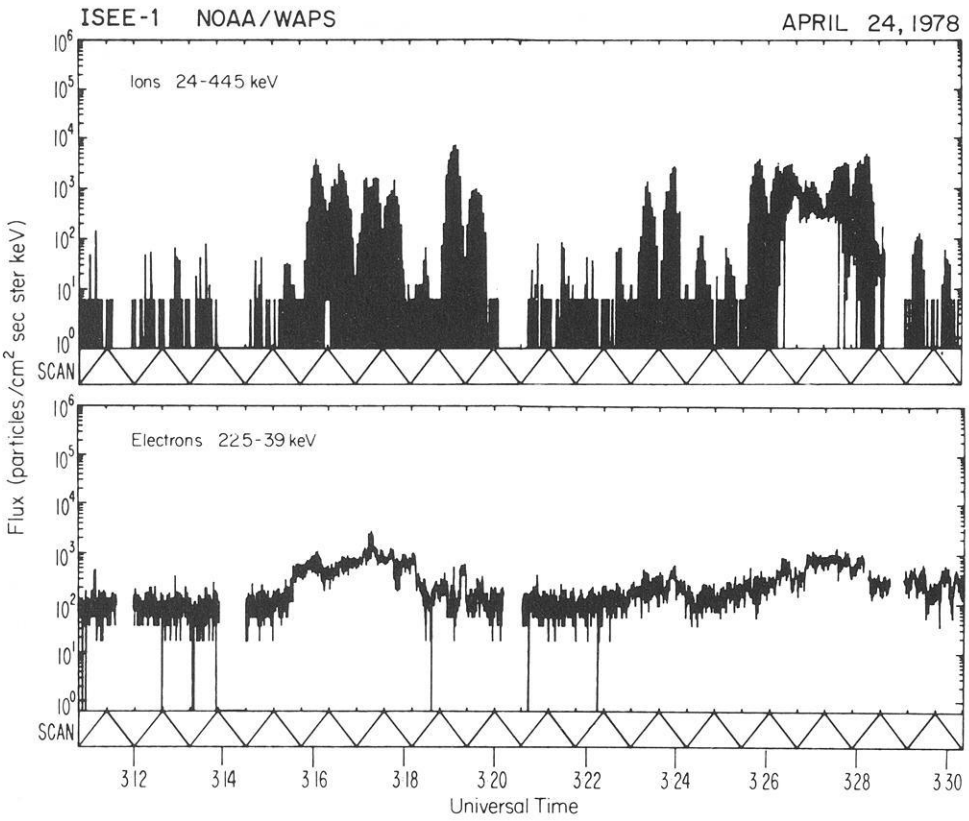


**Fig. 23.** High-resolution ion and electron observations from the lowest ion (24–44.5 keV) and electron 22.5–39 keV) channels for ISEE 1 on day 114 (April 24) 1978. The peaks are modulated by the scan motion, as indicated by the scan position at the bottom of each panel. Notice the difference between the three first peaks where look direction modulation from zero flux from the Earth to high flux from the tail direction is seen, and the fourth peak which shows shoulders of similar field alignment and an interior of nearly isotopic fluxes (little look direction modulation). (Lower panel). Corresponding electron observation shows no such distinct features (Spjeldvik and Fritz, 1981)

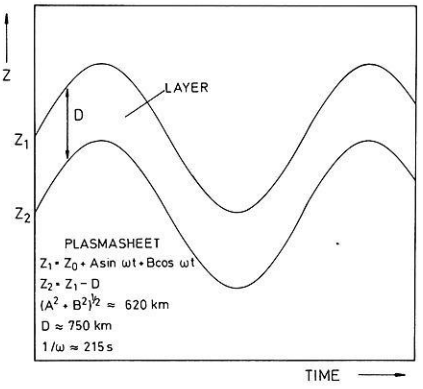


**Fig. 24.** Schematic representation of the plasma sheet boundary motion

lite is now beyond the boundary layer in the interior of the plasma sheet.

Spjeldvik and Fritz (1981) have interpreted the multiple crossings of the energetic ion layer in terms of large-scale waves of the boundary superimposed on the general plasma sheet thickening associated with the substorm process. Assuming that these waves are not travelling along the plasma sheet boundary but are only normal to the plasma sheet surface, the distance of the flow layer-lobe transition from the neutral sheet can be described by a sinusoid in time superimposed on the unperturbed surface position (see Fig. 24). The same holds for the flow layer-plasma sheet interior transition which is supposed to have a distance $D$ from the lobe-flow layer transition. From the data for the last crossing shown in Fig. 23, Spjeldvik and Fritz (1981) obtain a layer thickness of 750 km, a wave amplitude of $\sim$620 km and a wave period of $\sim$216 s.

## Conclusions

Energetic particles have been used successfully in order to study magnetospheric boundaries like the magnetopause and the plasma sheet boundary. Such studies require ideally high temporal and good energy and angular resolution and $4\pi$ coverage. The diagnostic value of energetic particles lies in the fact that due to their large gyroradii these particles can probe magnetospheric boundaries to larger distances. Such measurements have revealed the "wavy" structure of the magnetopause. Furthermore, by using energetic ions of magnetospheric origin as field line tracers the magnetic field topology near magnetospheric boundaries can be inferred.

It cannot be determined from energetic particle measurements alone whether the magnetopause is a rotational or tangential discontinuity. However, the observation of certain signatures of energetic particles near the magnetopause has added confidence to the identification of reconnection events. Similarly, the observation of energetic magnetospheric ions in flux transfer events has given strong support to the suggestion that these are flux tubes interconnected with the geomagnetic field.

The magnetic field near the magnetopause can change magnitude and direction over one gyroradius of an energetic ion. This is particularly true close to an $x$-type neutral line in a reconnection configuration or when magnetosheath field lines are draped around a flux tube connected with the magnetospheric field. In order to make further use of energetic ions as topology tracers their nonadiabatic behaviour in such magnetic field configuration has to be studied. Important contributions in this respect have been given by Speiser et al. (1981), Speiser and Williams (1982) and Daly (1983).

Magnetospheric ions are not only observed in the magnetosheath during reconnection events or in flux transfer events but are a more common feature outside the magnetopause. Their occurrence leads to several new questions which have not been attacked so far. In particular, it might be possible that while plasma and field measurements rely on the local occurrence of reconnection, energetic magnetospheric particles in the magnetosheath may be a signature of reconnection occurring much further away from the measuring site. A statistical analysis of their occurrence pattern may give important information about the magnetopause on a more global basis.

The energetic ion beams at the edge of the plasma sheet are of great importance for the process of plasma sheet recovery following magnetospheric substorms. It has been suggested that the thickening of the plasma sheet during recovery is caused by the populating of field lines previously devoid of energetic plasma with new particles from the neutral line region in the distant tail. Due to the tailward retreat of the neutral line and the continuous reconnection process, the plasma sheet builds up and thickens. Detailed study of the energetic ion beams may shed light on the origin of the plasma sheet.

## References


Andrews, M.K., Keppler, E., Daly, P.W.: Plasma sheet motions inferred from medium-energy ion measurements. J. Geophys. Res. **86**, 7543–7556, 1981a

Andrews, M.K., Daly, P.W., Keppler, E.: Ion jetting at the plasma sheet boundary: simultaneous observations of incident and reflected particles. Geophys. Res. Lett. **8**, 987–990, 1981b

Baker, D.N., Stone, E.C.: The magnetopause electron layer along the distant magnetotail. Geophys. Res. Lett. **4**, 133–136, 1977

Daly, P.W., Williams, D.J., Russell, C.T., Keppler, E.: Particle signature of magnetic flux transfer events at the magnetopause. J. Geophys. Res. **86**, 1628–1632, 1981

Daly, P.W., Fritz, T.A.: Trapped electron distributions on open magnetic field lines. J. Geophys. Res. **87**, 6081–6088, 1982

Daly, P.W., Keppler, E.: Observation of a flux transfer event on the earthward side of the magnetopause. Planet. Space Sci. **30**, 331–337, 1982

Daly, P.W.: Remote sensing of energetic particle boundaries. Geophys. Res. Lett., in press, 1983

Domingo, V., Page, D.E., Wenzel, K.P.: Energetic relativistic electrons near the polar magnetopause. J. Geophys. Res. **82**, 2327–2336, 1977

Eastman, T.E., Frank, L.A.: Observations of high-speed plasma flow near the Earth's magnetopause: evidence for reconnection? J. Geophys. Res. **87**, 2187–2201, 1982

Fahnenstiel, S.C.: Standing waves observed at the dayside magnetopause. Preprint, NOAA-ERL, Boulder, Colorado, 1981

Fritz, T.A., Fahnenstiel, S.C.: High temporal resolution energetic particle soundings at the magnetopause on November 8, 1977, using ISEE 2. J. Geophys. Res. **87**, 2125–2131, 1982

Forbes, T.G., Hones, E.W., Bame, S.J., Asbridge, J.R., Paschmann, G., Schopke, N., Russell, C.T.: Evidence for the tailward retreat of a magnetic neutral line in the magnetotail during substorm recovery. Geophys. Res. Lett. **8**, 261–264, 1981

Kaufmann, R.L., Konradi, A.: Explorer 12 magnetopause observations: Large-scale nonuniform motion. J. Geophys. Res. **74**, 3609–3627, 1969

Kaufmann, R.L., Konradi, A.: Speed and thickness of the magnetopause. J. Geophys. Res. **78**, 6549–6568, 1973

Konradi, A., Kaufmann, R.L.: Evidence for rapid motion of the outer boundary of the magnetosphere. J. Geophys. Res. **70**, 1627–1637, 1965

Krimigis, S.M., Sarris, E.T.: Energetic particle bursts in the Earth's magnetotail. In: Dynamics of magnetosphere, S.-I. Akasofu, ed.: pp 599–630, Dordrecht: D. Reidel Publ. Co. 1979

Lanzerotti, L.J., Krimigis, S.M., Bostrom, C.O., Axford, W.I., Lepping, R.P., Ness, N.F.: Measurements of the plasma flow at the dawn magnetopause by Voyager 1. J. Geophys. Res. **84**, 6483–6488, 1979

Meng, C.-I., Anderson, K.A.: Characteristics of the magnetopause energetic electron layer. J. Geophys. Res. **80**, 4237–4243, 1975

Möbius, E., Ipavich, F.M., Scholer, M., Gloeckler, G., Hovestadt, D., Klecker, B.: Observations of a nonthermal ion layer at the plasma sheet boundary during substorm recovery. J. Geophys. Res. **85**, 5143–5148, 1980

Paschmann, G., Sonnerup, B.U.Ö., Papamastorakis, I., Sckopke, N., Haerendel, G., Bame, S.J., Asbridge, J.R., Gosling, J.T., Russell, C.T.: Plasma acceleration at the Earth's magnetopause: evidence for reconnection. Nature **282**, 243–246, 1979

Richter, A.K., Keppler, E., Axford, W.I., Denskat, K.U.: Dynamics of low energy electrons (>17 keV) and ions (>80 keV) in the vicinity of the low-latitude duskside magnetopause: Helios 1 and 2 observations. J. Geophys. Res. **84**, 1453–1463, 1979

Russell, C.T., Elphic, R.C.: Initial ISEE magnetometer results: magnetopause observations. Space Sci. Rev. **22**, 681–715, 1978

Russell, C.T., Elphic, R.C.: ISEE observations of flux transfer events at the dayside magnetopause. Geophys. Res. Lett. **6**, 33–36, 1979

Scholer, M., Ipavich, F.M., Gloeckler, G., Hovestadt, D., Klecker, B.: Leakage of magnetospheric ions into the magnetosheath along reconnected field lines at the dayside magnetopause. J. Geophys. Res. **86**, 1299–1304, 1981

Scholer, M., Daly, P.W., Paschmann, G., Fritz, T.A.: Field line topology determined by energetic particles during a possible magnetopause reconnection event. J. Geophys. Res. **87**, 6073–6080, 1982a

Scholer, M., Hovestadt, D., Ipavich, F.M., Gloeckler, G.: Energetic protons, alpha particles, and electrons in magnetic flux transfer events. J. Geophys. Res. **87**, 2169–2175, 1982b

Scholer, M., Ipavich, F.M.: Interaction of ring current ions with the magnetopause. J. Geophys. Res., 1983

Sonnerup, B.U.Ö., Paschmann, G., Papamastorakis, I., Sckopke, N., Haerendel, G., Bame, S.J., Asbridge, J.R., Gosling, J.T., Russell, C.T.: Evidence for magnetic field reconnection at the Earth's magnetopause. J. Geophys. Res. **86**, 10049–10067, 1981

Speiser, T., Williams, D.J., Garcia, H.: Magnetically trapped ions as a source of magnetosheath energetic ions. J. Geophys. Res. **86**, 723–732, 1981

Speiser, T., Williams, D.J.: Magnetopause modelling: flux transfer events and magnetosheath quasi-trapped distributions. J. Geophys. Res. **87**, 2177–2186, 1982

Spjeldvik, W.N., Fritz, T.A.: Energetic ion and electron observations of the geomagnetic plasma sheet boundary layer: Three-dimensional results from ISEE 1. J. Geophys. Res. **86**, 2480–2486, 1981

Williams, D.J.: Magnetopause characteristics inferred from three-dimensional energetic particle distributions. J. Geophys. Res. **84**, 101–104, 1979a

Williams, D.J.: Observations of significant magnetosheath anti-solar energy flow. J. Geophys. Res. **84**, 2105–2108, 1979b

Williams, D.J., Frank, L.A.: ISEE-1 charged particle observations indicative of open field lines near the subsolar region. J. Geophys. Res. **85**, 2037–2042, 1980

Williams, D.J.: Magnetopause characteristics at 0840–1040 hours local time. J. Geophys. Res. **85**, 3387–3395, 1980

Williams, D.J.: Energetic ion beams at the edge of the plasma sheet – ISEE 1 observations plus a simple explanatory model. J. Geophys. Res. **86**, 5507–5518, 1981


Received October 8, 1982; Revised version November 29, 1982
Accepted November 30, 1982